Human & Experimental Toxicology

Inhibition of circRTN4 attenuates myocardial ischemia/reperfusion injury via the miR-185-5p/PHLPP2 axis

Journal:	*Human and Experimental Toxicology*
Manuscript ID	HET-25-0314
Manuscript Type:	Original Research Article
Date Submitted by the Author:	21-Jul-2025
Complete List of Authors:	Yin, Congcong ; Taizhou First People's Hospital Yan, Yunbo; Taizhou First People's Hospital,
Keyword:	myocardial ischemia, reperfusion injury, circRTN4, miR-185, PHLPP2

Abstract:

Introduction:
Myocardial ischemia-reperfusion injury (MIRI) occurs in the heart muscle when the blood supply is temporarily interrupted and restored. The oxidative stress and inflammatory response induced during the ischemia phase is exacerbated during the reperfusion duration, while reperfusion is necessary to maintain the normal function of the heart and all other organs. Limited studies have been conducted to understand how circRNAs regulate miRNA during ischemia-reperfusion injury.
In this study, we hypothesize that inhibition of circRTN4 attenuates the oxidative stress, and inflammatory responses in heart tissue via the miR-185-PHLPP2 axis.
Methods:
We applied both in vivo and in vitro models: oxygen-glucose deprivation/reperfusion (OGD/R) model in HL-1 cells and MIRI in mice, with or without transfection of si-circRTN4, miR-185 inhibitor, and PHLPP2 ORF-clone.
Results:
After OGD/R induction, decreased cellular viability was noticed in HL-1 cells while inhibiting the expression of circRTN4, attenuating the injury. Similarly, the increased inflammatory cytokines: TNFα, IL-1β, and IL-18, and oxidative stress (ROS and MDA), and decreased trends were noticed in anti-oxidative stress marker: SOD, and anti-inflammatory cytokine: IL-10, were noticed in HL-1 cells after OGD/R. Silencing of circRTN4 attenuated the oxidative stress and pyroptosis induced by OGD/R. Moreover, knocking down the miR-185 or PHLPP2 overexpression diminished the protection effects from circRTN4 silencing. Similar dysregulation trends were observed in mice MIRI model. Our results provide a novel insight into the molecular mechanism involved in MIRI that inhibition of circRTN4 attenuates the heart tissue injury via the miR-185-PHLPP2 axis.

Inhibition of circRTN4 attenuates myocardial ischemia/reperfusion injury via the miR-185-5p/PHLPP2 axis

Running title: CircRTN4 aggravates MI/R injury

Congcong Yin, Yunbo Yan*

Authors' Affiliations: Emergency Department, Taizhou First People's Hospital, 218 Hengjie Road, Huangyan District, Taizhou 318020, Zhejiang, China.

*Correspondence to: Yunbo Yan, Yunboyan@163.com

Emergency Department, Taizhou First People's Hospital, 218 Hengjie Road, Huangyan District, Taizhou, Zhejiang 318020. +86-(0576)84120120.

Abstract

Introduction:

Myocardial ischemia-reperfusion injury (MIRI) occurs in the heart muscle when the blood supply is temporarily interrupted and restored. The oxidative stress and inflammatory response induced during the ischemia phase is exacerbated during the reperfusion duration, while reperfusion is necessary to maintain the normal function of the heart and all other organs. Limited studies have been conducted to understand how circRNAs regulate miRNA during ischemia-reperfusion injury. In this study, we hypothesize that inhibition of circRTN4 attenuates the oxidative stress, and inflammatory responses in heart tissue via the miR-185-PHLPP2 axis.

Methods:

We applied both in vivo and in vitro models: oxygen-glucose deprivation/reperfusion (OGD/R) model in HL-1 cells and MIRI in mice, with or without transfection of si-circRTN4, miR-185 inhibitor, and PHLPP2 ORF-clone.

Results:

After OGD/R induction, decreased cellular viability was noticed in HL-1 cells while inhibiting the expression of circRTN4, attenuating the injury. Similarly, the increased inflammatory cytokines: TNFα, IL-1β, and IL-18, and oxidative stress (ROS and MDA), and decreased trends were noticed in anti-oxidative stress marker: SOD, and anti-inflammatory cytokine: IL-10, were noticed in HL-1 cells after OGD/R. Silencing of circRTN4 attenuated the oxidative stress and pyroptosis induced by OGD/R. Moreover, knocking down the miR-185 or PHLPP2 overexpression diminished the protection effects from circRTN4 silencing. Similar dysregulation trends were observed in mice MIRI model.

Conclusion:

Our results provide a novel insight into the molecular mechanism involved in MIRI that inhibition of circRTN4 attenuates the heart tissue injury via the miR-185-PHLPP2 axis. More studies are

needed to fully understand the translation value of circRTN4 in preventing MIRI associated tissue damage.

Keywords: myocardial ischemia/reperfusion injury, circRTN4, miR-185, PHLPP2

Introduction:

Myocardial ischemia-reperfusion injury (MIRI) is a complex phenomenon that occurs in the cardiovascular with temporary blockage in blood vessels and then subsequently resolved (1). Usually, MIRI contains both ischemia and reperfusion phases, which ischemia induced by blood vessel blockage results in oxygen and nutrition reduction supplied by the blood (2). After resolving blood blockage, reperfusion occurs, which is necessary in rescuing the heart while also inducing heart damage and exacerbating the inflammation caused during the ischemia (3). Underlying MIRI, oxidative stress, and inflammation are the major molecular mechanisms discovered currently, and new insights into how molecular regulation can help prevent MIRI's post damage.

Circular RNA (circRNA) is one type of noncoding RNA with a closed-loop structure that helps enhance stability and prevent degradation from Rnase (4). CircRTN4, or circular RNA RTN4, is one type of circRNAs that regulate miRNA expression in different disease models. It has been proved that CircRTN4 promoted pancreatic cancer development through miR-497 regulated epithelial-mesenchymal transition (5). CircRTN4 also regulated the expression of miR-24 in promoting neurite growth (6). Another report also indicated that CircRTN4 delivered by mesenchymal stem cell secreted exosome helps to prevent the LPS induced inflammation and apoptosis in cardiomyocytes through miR-497-5p/MG53 axis (7). However, no study focused on the role of CircRTN4 in MIRI It is well known that circRNA contains lots of miRNA binding sites, which can inhibit multiple miRNAs for regulating the downstream pathway (8).

Multiple circRNAs have shown correlations with MIRI by regulating miRNA and its downstream pathways. CircHIPK3 inhibited the expression of miR-124 and exacerbated the cellular cytotoxicity of myocardial cells after oxygen deprivation (9). Regulated miR-302a by circDdx60 also helped to prevent apoptosis in mouse cardiomyocytes (10). Another circRNA, CircNNT, helped to exaggerate the inflammation and apoptosis after MIRI (11). Although studies have focused on the role of circRNAs on MIRI, no study directly investigated how circRTN4 regulated the process of MIRI. Another miRNA, miR-185, positively prevented inflammation and oxidative stress during MIRI (12). Currently, no study focuses on the interaction between circRTN4 and miR-185 in preventing MIRI.

In this manuscript, we proposed to understand the role of circRTN4 in regulating the miR-185/PHLPP2 axis during MIRI-associated heart injury. A low level of miR-185 has been found after myocardial ischemia(13), and we propose that inhibiting the expression level of circRTN4 helps to restore the transcript level of miR-185, hence preventing the MIRI.

Method:

Animal model and MIRI establishment

All female C57BL/6 mice around 6-8 weeks old were purchased from Slack Laboratory Animal Co., Ltd. (Shanghai，China) and kept in animal vivarium with 12-h light/dark cycle at steady temperature and humidity for 1 week before the experiment. Six mice were used for each experimental group: Control, I/R，I/R+sh-NC，and I/R+sh-circRTN4. Before the myocardial

ischemia and reperfusion surgery, mice were anesthetized by 2% isoflurane with 98% oxygen. The ischemia procedure was induced by ligation of the left anterior descending artery (LAD) with a suture for 30 mins followed by reperfusion for 24 hrs as described in a previous publication (14). Customized sh-circRTN4 vector (15) mixed with Lipofectamine 3000 transfection reagent (Cat#: L3000150, Thermofisher) was injected into the heart tissue before the surgery and allowed 3 days for transfection. After 24 hrs reperfusion, mice were sacrificed by overdosing of ketamine/xylazine and performed cervical dislocation, blood and heart tissues were collected for further analysis. Experimental protocol applied in this study was approved by the Animal Ethics Committee of the First People's Hospital of Taizhou. The study is reported in accordance with ARRIVE guidelines (https://arriveguidelines.org).

Cell culture and treatment

Mouse cardiac muscle cell line (HL-1) was purchased from EMDMillipore (Cat#: SCC065), and maintained in claycomb medium (Cat#: 51800C, Sigma) with 2mM L-glutamine, 1x penicillin-streptomycin, 100μM norepinephrine, and 10% FBS at 37°C with 5% CO_2 and 95% humidity. To establish the ischemia injury, OGD/R model was used as *in vitro* model: cells were washed with PBS, and then incubated with glucose-free DMEM (pre-incubate at 95% N_2, 5%CO_2 for 30mins to achieve oxygen and glucose deprivation. Then, cells were collected for further analysis. Overexpression of PHLPP2 was achieved by transfecting viral-particle packed with plasmids with PHLPP2-ORF-clone (Cat#: MR219729L3V, Origene) at 10 MOI. Transfection was conducted based on the manufacturer's protocol for 4 hrs and cells were recovered overnight. Circular RTN4 and miR-185 inhibitor and miR-185 mimic were purchased from IDT genes and transfected into cells by Lipofectamine 3000 (Cat#: L3000150, Thermofisher) per the manufacturer's protocol. After transfection, cells were incubated for 24 hrs for recovery, and then used for OGD/R model establishment and further analysis.

Cell viability measurement.

CCK8 kit was purchased from Abcam (Cat#: Ab228554) to measure cellular viability. Briefly, WST-8 (2-[2-methoxy-4-nitrophenyl]-3-[4-nitrophenyl]-5-[2,4-disulfophenyl]-2H-tetrazolium) solution was added to the cells after treatment and incubated for 45 mins, and the absorbance at OD460 was measured. Blank wells were used as negative control.

RNA isolation and qRT-PCR

Heart tissue or cells were lysed in QIAzol reagent (Cat#:79306, Qiagen) for 30 mins and then mixed with chloroform for 15 s. The mixture was centrifuged at 20000 g for 30 mins at 4°C. The aqueous phase was collected and mixed thoroughly with isopropanol for 2 hrs at -20 °C. Then, the mixtures were spun down at 15,000 g for 30 min at 4 °C, and washed with 75% EtOH once. The samples were centrifuged at 20000 × g for 30 min at 4 °C, and then removed the EtOH. RNA pellets were resuspended by 50μl of RNase-free water. RNA concentrations were quantified by Nano-drop spectrophotometer (ND-1000, NanoDrop Technologies). Total 200 ng RNA was prepared for each sample for qRT-PCR analysis. First, RNA was applied to reverse transcription (RT) by TaqMan™ Reverse Transcription Reagents (Cat# N8080234, Thermofisher) and quantitative real-time PCR (qPCR) based on TaqMan™ Fast Advanced Master Mix for qPCR (Cat#: 4444557, Thermofisher). PHLPP2 (Assay ID: Mm01244270_m1, Thermofisher) was purchased, and circRTN4 probes were customized from the thermofisher. GAPDH (Assay ID:

Mm99999915_g1, Thermofisher) was used as housekeeping control for PHLPP2 and circRTN4. The primer and probe for MiR-185-5p (assayID: Mm04238131_s1, Thermofisher) and snoRNA135 (assay ID: 001230, Thermofisher) were applied in both RT and qPCR, and snoRNA135 was used as endogenous control for normalization of miR-185. For reverse transcription, the mixture was incubated at 16°C for 30mins, then 42°C for 30mins, and the reaction was stopped for 5 mins at 85 °C. The samples were kept at 4°C for qPCR. For qPCR, the mixtures were incubated at 50°C for 2 mins, and 95°C for 10 mins, then 40 cycles of 95°C for 10 s, and 60 °C for 1 min, and fluorescence intensity was checked at the end of 60°C incubation duration, for 40 times. The change fold was calculated by $2^{-\Delta\Delta Ct}$ method.

Protein isolation and Western blot

Snap-frozen heart tissue or cells were lysed in RIPA buffer with a protease inhibitor. Protein concentrations were measured by Pierce BCA Assay Kit (Cat#: 23227, Thermo Fisher Scientific). Total protein (15 µg) was used for immune-blotting. Proteins were separated by 10 % sodium dodecyl sulfate–polyacrylamide gel electrophoresis (SDS-PAGE), and then transferred to a nitrocellulose membrane by 100V, 1hr, at 4°C. Then, the membrane was blocked by 5% BSA, prepared in Tris-buffered saline containing 0.1% Tween 20 (TBS-T) 1 hr at room temperature. The membranes were incubated with primary antibodies: anti- NLRP3 (1: 1000, ab263899, Abcam), anti-caspase 1 (1:1000, ab179515, Abcam), IL-1β (1:1000, ab315084, Abcam), anti-GSDMD-N (1:1000, PA5-116815, Thermofisher) overnight at 4°C. The next day, membranes were washed and incubated with secondary antibody (goat-anti-rabbit, 1:10000, #1706515, BioRad) for 1 hr at room temperature. Then, membranes were developed by Pierce ECL Western Blotting Substrate (Cat#: 32106, Thermofisher Scientific), and detected by Bio-Rad ChemiDoc MP imaging system.

Measurement of ROS

The level of ROS was measured by the treatment with H_2DCF-DA kit purchased from Abcam (ab113851) based on the manufacturer's protocol. Briefly, cells were incubated with DCFDA reagent for 45 mins at 37°C in dark, and then the fluorescent intensity was measured at Excitation/Emission of 485/535 by a plate reader.

Measurement of MDA and SOD

The MDA assay kit (Cat: ab118970, Abcam) was used based on the protocol to measure the level of MDA. First, the MDA-TBA adduct was added to the sample mixture with the developer VII/TBA at 95°C for 60 mins. The mixture was used directly to measure the expression level of MDA at OD532. The SOD assay kit (Cat: ab211096, Abcam) was used to measure the level of SOD. After the treatment, cells were washed with PBS 2 times and then incubated with β-Galactosidase at 37°C for 10 mins in dark. The substrate solution was added to the mixtures, and incubated for 30 mins at 37°C. After incubation, sodium developer was added to each well. The absorbance was detected at the wavelength of 405 nm.

ELISA

The cell culture supernatant and serum from mice were centrifuged at 1000 g for 5 mins. The cytokine levels of TNF-α (Cat#MTA00B), IL-1β (Cat#MLB00C), and IL-18 (Cat#DY7625)

were measured from the supernatant by ELISA kit purchased from R&D system Inc, following the manufacturer's protocol. Blank wells served as negative controls.

Luciferase assay

The luciferase reporter containing circRTN4 and PHLPP2 plasmids were transfected into the cells one day before the experiment. Then, cells were transfected with miR-185 and miR-NC for 4 hrs. Luciferase assay solution (Cat#: ab228530, Abcam) was added to the cells and incubated for 20 mins at room temperature. The luminescence intensity was recorded by the luminometer. Blank wells were used to normalize the results and used as the background luminescence intensity

H&E staining

Sections (5μm) prepared from formalin fixed heart tissue was deparaffinized by xylene and rehydrated by 100%, 90%, 75% EtOH, and water. Then, sections were stained with hematoxylin for 1 min and rinsed with water for 5 mins. Sections were blued with 0.1% ammonia-water for 10 s, followed by washing with water for 10 mins. The sections were incubated with 95% EtOH for 2 mins and stained with Eosin for 1 min. Then the slides were dehydrated by EtOH and xylene, and then mounted for microscopy imaging.

Creatine kinase (CK-MB) measurement

The CK-MB test was conducted based on the ELISA kit purchased from Abcam (ab285231). The samples were added to the wells and incubated for 1.5 hrs at 37°C. Then, the samples were incubated with biotin-detection antibody for 1hr at 37°C. The plates were then ncubated with SABC solution for 30 mins at 37°C. Finally, the plate was developed with TMB substrate for 20 mins at 37°C in dark, and the plate was read at OD450.

LDH measurements

Mouse serum was used to measure the LDH level by LDH assay kit (Cat# ab102526, abcam). Serum samples were added to the wells and mixed with LDH assay buffer and substrate. The plates were incubated at 37°C for 30 mins and the plate was read at OD450.

Statistical analysis:

All experiments were independently performed at least three times. Data was presented as mean±SD. All the significant difference was calculated by one-way ANOVA with Tukey post hoc comparison or student's t-test via GraphPad Prism software (V.10.0). $p < 0.05$ was considered as significant.

Results:

Inhibiting the circRTN4 level restored the cell viability and reduced the ROS level in HL-1 cells after OGD/R

HL-1 cells were deprived of oxygen and glucose as an *in vitro* ischemia model. After OGD/R treatment, HL-1 cells showed higher level of circRTN4 compared to the control group (Fig 1A). After transfection of si-circRTN4 into the HL-1 cells, the induction of circRTN4 gene expression after OGD/R was inhibited in the OGD/R+si-circRTN4 group compared to the OGD/R group (Fig 1B). Besides the gene level of circRTN4, cellular proliferation was inhibited after OGD/R as well, while inhibiting circRTN4 showed recovery in cell viability compared to the OGD/R group (Fig 1C). Agreed with inhibited cellular proliferation, treatment of OGD/R showed

increased oxidative stress compared to the control group, while transfection of si-circRTN4 showed less oxidative than the OGD/R-only group (Fig 1D). The level of SOD showed decreased after treatment of OGD/R and recovered after silencing of circRTN4, while the level of MDA was opposited to SOD under individual group (Fig 1E).

Suppression of the circRTN4 alleviates OGD/R-induced pyroptosis in HL-1 cells.

The decreased cell viability of HL-1 cells induced by OGD/R was inhibited by suppression of circRTN4 (Fig 1), and the oxidative stress and inflammatory response caused by OGD/R was also attenuated by silencing the expression of circRTN4 (Fig 2). After OGD/R, protein expression levels of pyroptosis markers, cleaved caspase 1 and GSDMD-N were increased compared to control group, and partially reduced upon si-circRTN4 transfection (Fig 2A). Similarly, the activities of caspase-1 and -4 were increased after OGD/R and decreased after si-circRTN4 treatment (Fig 2B). The pyroptosis related-inflammatory cytokines (TNFα, IL-1β, and IL-18) showed increased levels after OGD/R treatment while inhibited after silencing of circRTN4, and the anti-inflammatory cytokine, IL-10, showed the opposite the trend (Fig 2C). These results suggested that suppression of the circRTN4 had alleviated OGD/R-induced pyroptosis in HL-1 cells.

OGD/R induced upregulation of CircRTN4 targeting on the expression of miR-185-5p and PHLPP2 in HL-1 cells.

Throughout the starBase prediction (https://bio.tools/starbase), the miR-185-5p was the direct target of circRTN4 (Fig 3A). HL-1 cells with luciferase reporter on circRTN4 proved that overexpression of miR-185 inhibited the luciferase activity (Fig 3B). Based on the starBase prediction, miR-185-5p directly regulated the level of PHLPP2, and the luciferase activity in HL-1 cells showed that miR-185-5p transfection inhibiting the PHLPP2 associated luciferase activity (Fig 3C). The RNA immunoprecipitation (RIP) qRT-PCR showed that HL-1 cells showed AGO2 protein were more interacted with circRTN4 and miR-185 compared to the negative control (IgG group) (Fig 3D). After treatment of OGD/R, HL-1 cells showed a significant decrease in miR-185 (Fig 3E), and the same downregulation was noticed after transfection of anti-miR-185-5p (Fig 3F). The protein expression level of PHLPP2 was increased after induction of OGD/R, while decreased PHLPP2 level was found after circRTN4 silencing (Fig 3G). An increased level of PHLPP2 protein was noticed in the OGD/R+si-circRTN4+miR-185-5p inhibitor group compared to the OGD/R+si-circRTN4 group (Fig 3G). The results demonstrated that miR-185 regulating the expression of PHLPP2 might be the potential signaling pathway under circRTN4 during OGD/R induced cytotoxicity.

CircRTN4 regulated the OGD/R-induced cytotoxicity and pyroptosis in HL-1 cells through the miR-185-PHLPP2 axis.

Transfection of PHLPP2-ORF-clone showed a higher protein level of PHLPP2 compared to other showed the successful establishment of the overexpression system (Fig 4A). The cell viability of HL-1 cells was inhibited after induction of OGD/R, while knockdown of circRTN4 helped to recover the cell growth (Fig 4B). Transfection of anti-miR-185 or overexpression of

PHLPP2 increased the cytotoxocuty induced by OGD/R compared to the OGD/R+si-circRTN4 group (Fig 4B). OGD/R induced oxidative stress in HL-1 cells were also noticed to correlate with the levels of miR-185 and PHLPP2. Silencing circRTN4 helped to decrease the ROS level while anti-miR-185 or PHLPP2 overexpression both upregulated ROS level (Fig 4C). The protein expression levels of cleaved caspase-1 and GSDMD-N were increased after OGD/R treatment, while knockdown of circRTN4 help to reduce the overepxression of both protein expressions (Fig 4D). The anti-miR-185 or overexperssion of PHLPP2 overcomed the inhibition of cleaved caspase-1 and GSDMD-N induced by si-circRTN4 transfection (Fig 4D). The same trend among different condition groups were noticed in the activities of caspase-1 and -4 (Fig 4E). The inflammatory cytokines: TNF-α, IL-1β, and IL-18, showed increased after OGD/R, while inhibited by si-circRTN4 via miR-185-PHLPP2 axis (Fig 4F).

Inhibition of circRTN4 alleviates MIRI in mice via miR-185-PHLPP2 axis

Mice challenged after ischemia and reperfusion showed increased levels of CK-MB and LDH compared to the sham group, and inhibiting the expression of circRTN4 in heart tissue helped to reduce the level of CK-MB and LDH (Fig 5A). As expected, the gene expression levels of circRTN4 and PHLPP2 were increased and decreased miR-185 gene level in the I/R group compared to sham group. The knockdown of circRTN4 helped to reduce the overexpression of circRTN4 and PHLPP2 and restored the expression of miR-185 compared to the I/R group (Fig 5B). After ischemia and reperfusion, the heart tissue showed myocardial damage visualized by H&E staining, while knockdown of circRTN4 attenuated the tissue damage (Fig 5C). The serum MDA level showed increased after I/R while decreased after circRTN4 silencing (Fig 5D). The protein expressions of cleaved caspase-1 and GSDMD-N were upregulated after I/R, and circRTN4 inhibition brought down the protein levels (Fig 5E). Similarly, the activities of caspase-1 and -4 were induced after I/R and inhibited by the circRTN4 knockdown (Fig 5F). The inflammatory cytokines (TNF-α, IL-1β, and IL-18) from mouse serum were upregulated after I/R treatment and silencing circRTN4 helped to reduce upregulated cytokin levels (Fig 5F-G). The animal experiments proved the previous in vitro results that circRTN4 silencing could be one of the therapeutic methods in MIRI induced oxdative stress, inflammation response and pyroptosis.

Discussion:

MIRI is a significant challenge in cardiovascular disease (CVD), and is currently the leading cause of CVD-induced death globally (16). It is well known that MIRI is associated with oxidative stress and inflammatory responses in the cardiovascular system, which could lead to the worsening of heart injury resulting from myocardial infarction (17, 18). CircRNAs have been shown in previous literature that correlated with MIRI development by targeting different miRNAs (19). In this manuscript, HL-1 cells showed increased expression level of circRNT4 after oxygen and glucose deprivation, and the same trend showed in the heart tissue of the mice challenged with ischemia and reperfusion. Knockdown of circRTN4 showed potential in protecting the MIRI-associated tissue damage, oxidative stress, and inflammatory responses. One possible mechanism involved with the dysregulation of circRTN4 is the miR-185-PHLPP2 axis, which shares the direct binding site of miR-185 to circRTN4, and PHLPP2 is the downstream target of miR-185.

CircRNAs have been shown that correlated with cardiomyocyte injury and cytotoxicity. Overexpression of circHIPK2 promoted cardiomyocyte apoptosis caused by oxidation via regulating the miR-485- ATG101 axis (20). Another circRNAs, circNCX1, also served as an miR-133 inhibitor in cardiomyocytes to regulate cellular apoptosis and oxidative stress (21). The overexpression of circNFIX showed potential regulation on the miR-125-TLR4 axis in regulating cellular apoptosis and oxidative stress in either cardiomyocytes or heart tissue from mice challenged by ischemia and reperfusion (22, 23). This study provided a new insight that circRTN4 regulated miR-185-PHLPP2 axis in cellular oxidative stress and inflammatory response caused by ischemia and reperfusion injury in either cardiomyocytes or *in vivo* mode. Except for the circRNAs in regulating cellular apoptosis, other circRNAs were associated with MIRI related damage. CircSAMD4A exacerbated the heart tissue damage after hypoxia and reoxygenation via regulating miR-138 expression (24). The circRNA MFACR promotes the MIRI induced tissue injury and cardiomyocytes cytotoxicity through miR-652 (25).

Similarly, circ0060745 and circ010567 exaggerated the cardiomyocyte apoptosis upon the ischemia occurrence (26, 27). Mostly reported circRNAs were positively correlated with heart tissue damage development after ischemia and reperfusion. This manuscript pointed out that inhibiting the expression of circRTN4 helped restore the level of miR-185, which inhibited the PHLPP2 transcript level and helped reduce the oxidative stress, and pyroptosis caused by lack of oxygen and nutrition. This study is the first to show circRTN4 was involved in the ischemia-induced cell apoptosis.

There is limited study on circRTN4 in CVDs, and not even one focused on how circRTN4 regulated MIRI. Although limited studies are available currently, most studies investigated the correlation of circRTN4 with miRNAs and it's downstream pathway. CircRTN4 has been shown to promote pancreatic cancer development through miR-497 expression and epithelial-mesenchymal transition (5). CircRTN4 also helped to promote neurite growth via regulating miR-24 (6). Our results showed that overexpression of circRTN4 could inhibit the cellular proliferation of cardiomyocytes and increase cell death compared to the control group. It might be the tissue or cell types differences. Also, exosomal circRTN4 secreted from mesenchymal stem cells helped to

protect LPS induced inflammation and apoptosis in cardiomyocytes (7). In this manuscript, knocking down circRTN4 in cardiomyocytes helped prevent inflammation, which disagreed with previous literature. Although there is disagreement about the circRTN4 in anti-inflammatory and anti-apoptosis in cardiomyocytes, the inducer differs from the literature for our study. Ischemia induced inflammation and apoptosis could be more complicated with the involvement of multiple pathways. A thorough study is needed to understand the role of circRTN4 in inflammation and the difference in different inflammation models.

In this study, the expression of miR-185 was significantly inhibited when ischemia occurred and restored after silencing circRTN4. It has been well studied that miR-185 is a potential target in CVDs. The level of miR-185 in serum was higher in patients suffered from right ventricular cardiomyopathy (28). An elevated level of miR-185 was also observed in patients with myocardial injury and disease toward remodeling (29). Another study showed that miR-185 overexpression promoted the development of myocardial fibrosis (30). However, not all the published studies demonstrated that miR-185 was upregulated during heart injury. The inhibition of miR-185 has been noticed to exacerbate the heart injury caused by infarction (13). The results provided in this study also proved that miR-185 inhibited ischemia induced injury, and inhibiting the expression of miR-185 exacerbated the damage. Another study showed that miR-185 was involved with CDK6 in MIRI induced pyroptosis, and inhibiting miR-185 expression exacerbated the heart cell apoptosis and inflammation (12). Our results agreed with the previous study that miR-185 is necessary in ischemia/reperfusion induced injury and inflammatory response, and loss of miR-185 could exaggerate the injury. Similarly, another study showed increased expression level of miR-185 helped restore the MIRI associated injury and inflammation, which agreed with the results provided in this study (31).

While the study provided valuable insights, certain limitations should be noticed. The conflict of miR-185 expression in different types of heart injury should be a concern of applying it as a potential medicine in MIRI. Additionally, exploring the downstream targets of miR-185 and circRTN4 other than PHLPP2 could help better understand the molecular mechanism and validate this finding. Some human subject samples can also help to understand the translational value of the circRTN4-miR185 axis in MIRI.

In conclusion, circRTN4 was upregulated after ischemia, and silencing of circRTN4 attenuated the heart tissue injury and HL-1 cell apoptosis. Overexpression of circRTN4 after MIRI inhibited the miR-185 levels which is necessary in preventing the heart tissue injury and inflammation after MIRI (Figure 6). This manuscript presented the significance of the circRTN4-miR-185-Phlpp2 axis in cellular responses during MIRI.

Author Declarations

Funding

Not applicable.

Conflicts of interest/Competing interests

Every author specified that there is no interest conflict.

Availability of data and material

Not applicable.

Code availability

Not applicable.

Authors' contributions

Congcong Yin and Yunbo Yan were responsible for study concept and design, acquisition of data, statistical analysis, interpretation of data, drafting of the manuscript, critical revision of the manuscript for important intellectual content, and approval of the final draft manuscript.

Ethics approval

This experiment was approved by the Animal Ethics Committee of the First People's Hospital of Taizhou. The study is reported in accordance with ARRIVE guidelines (https://arriveguidelines.org).

Consent to participate

Not applicable.

Consent for publication

Not applicable.

Acknowledgements

Not applicable.

References

1. Sánchez-Hernández CD, Torres-Alarcón LA, González-Cortés A, Peón AN. Ischemia/Reperfusion Injury: Pathophysiology, Current Clinical Management, and Potential Preventive Approaches. Mediators Inflamm. 2020;2020:8405370.
2. He J, Liu D, Zhao L, Zhou D, Rong J, Zhang L, et al. Myocardial ischemia/reperfusion injury: Mechanisms of injury and implications for management (Review). Exp Ther Med. 2022;23(6):430.
3. Kalogeris T, Baines CP, Krenz M, Korthuis RJ. Cell biology of ischemia/reperfusion injury. Int Rev Cell Mol Biol. 2012;298:229-317.
4. Patop IL, Wüst S, Kadener S. Past, present, and future of circ RNA s. The EMBO journal. 2019;38(16):e100836.
5. Wong CH, Lou UK, Fung FK, Tong JHM, Zhang CH, To KF, et al. CircRTN4 promotes pancreatic cancer progression through a novel CircRNA-miRNA-lncRNA pathway and stabilizing epithelial-mesenchymal transition protein. Mol Cancer. 2022;21(1):10.
6. Qi Y, Ma N, Chen X, Wang Y, Zhang W, Wan J. CircRtn4 Acts as the Sponge of miR-24-3p to Promote Neurite Growth by Regulating CHD5. Front Mol Neurosci. 2021;14:660429.
7. Li J, Jiang R, Hou Y, Lin A. Mesenchymal stem cells-derived exosomes prevent sepsis-induced myocardial injury by a CircRTN4/miR-497-5p/MG53 pathway. Biochem Biophys Res Commun. 2022;618:133-40.
8. Zheng Q, Bao C, Guo W, Li S, Chen J, Chen B, et al. Circular RNA profiling reveals an abundant circHIPK3 that regulates cell growth by sponging multiple miRNAs. Nat Commun. 2016;7:11215.
9. Bai M, Pan C-L, Jiang G-X, Zhang Y-M, Zhang Z. CircHIPK3 aggravates myocardial ischemia-reperfusion injury by binding to miRNA-124-3p. European Review for Medical & Pharmacological Sciences. 2019;23(22).
10. Sun Y, Zhang Y, Ye Z, Wang Y, Lao Y, Zhang J, et al. circRNA-miRNA Complex Participates in the Apoptosis of Myocardial Cells in Myocardial Ischemia/Reperfusion Injury. Discovery Medicine. 2022;33(168):13-26.
11. Ye X, Hang Y, Lu Y, Li D, Shen F, Guan P, et al. CircRNA circ-NNT mediates myocardial ischemia/reperfusion injury through activating pyroptosis by sponging miR-33a-5p and regulating USP46 expression. Cell Death Discovery. 2021;7(1):370.
12. Sun J, Zhu YM, Liu Q, Hu YH, Li C, Jie HH, et al. LncRNA ROR modulates myocardial ischemia-reperfusion injury mediated by the miR-185-5p/CDK6 axis. Lab Invest. 2022;102(5):505-14.
13. Li CC, Qiu XT, Sun Q, Zhou JP, Yang HJ, Wu WZ, et al. Endogenous reduction of miR-185 accelerates cardiac function recovery in mice following myocardial infarction via targeting of cathepsin K. J Cell Mol Med. 2019;23(2):1164-73.
14. Merx MW, Gorressen S, van de Sandt AM, Cortese-Krott MM, Ohlig J, Stern M, et al. Depletion of circulating blood NOS3 increases severity of myocardial infarction and left ventricular dysfunction. Basic Res Cardiol. 2014;109(1):398.
15. Wong CH, Lou UK, Fung FK-C, Tong JHM, Zhang C-h, To K-F, et al. CircRTN4 promotes pancreatic cancer progression through a novel CircRNA-miRNA-lncRNA pathway and stabilizing epithelial-mesenchymal transition protein. Molecular Cancer. 2022;21(1):10.
16. Zagidullin N, Motloch LJ, Gareeva D, Hamitova A, Lakman I, Krioni I, et al. Combining Novel Biomarkers for Risk Stratification of Two-Year Cardiovascular Mortality in Patients with ST-Elevation Myocardial Infarction. J Clin Med. 2020;9(2).

17. Venkatachalam K, Prabhu SD, Reddy VS, Boylston WH, Valente AJ, Chandrasekar B. Neutralization of interleukin-18 ameliorates ischemia/reperfusion-induced myocardial injury. J Biol Chem. 2009;284(12):7853-65.
18. Yeung HM, Hung MW, Lau CF, Fung ML. Cardioprotective effects of melatonin against myocardial injuries induced by chronic intermittent hypoxia in rats. J Pineal Res. 2015;58(1):12-25.
19. Wen ZJ, Xin H, Wang YC, Liu HW, Gao YY, Zhang YF. Emerging roles of circRNAs in the pathological process of myocardial infarction. Mol Ther Nucleic Acids. 2021;26:828-48.
20. Zhou J, Li L, Hu H, Wu J, Chen H, Feng K, et al. Circ-HIPK2 Accelerates Cell Apoptosis and Autophagy in Myocardial Oxidative Injury by Sponging miR-485-5p and Targeting ATG101. J Cardiovasc Pharmacol. 2020;76(4):427-36.
21. Li M, Ding W, Tariq MA, Chang W, Zhang X, Xu W, et al. A circular transcript of ncx1 gene mediates ischemic myocardial injury by targeting miR-133a-3p. Theranostics. 2018;8(21):5855-69.
22. Cui X, Dong Y, Li M, Wang X, Jiang M, Yang W, et al. A circular RNA from NFIX facilitates oxidative stress-induced H9c2 cells apoptosis. In Vitro Cell Dev Biol Anim. 2020;56(9):715-22.
23. Wang X, Sun Q, Hu W. Carvedilol Protects Against the H2O2-induced Cell Damages in Rat Myoblasts by Regulating the Circ_NFIX/miR-125b-5p/TLR4 Signal Axis. J Cardiovasc Pharmacol. 2021;78(4):604-14.
24. Hu X, Ma R, Cao J, Du X, Cai X, Fan Y. CircSAMD4A aggravates H/R-induced cardiomyocyte apoptosis and inflammatory response by sponging miR-138-5p. J Cell Mol Med. 2022;26(6):1776-84.
25. Wang K, Gan TY, Li N, Liu CY, Zhou LY, Gao JN, et al. Circular RNA mediates cardiomyocyte death via miRNA-dependent upregulation of MTP18 expression. Cell Death Differ. 2017;24(6):1111-20.
26. Bai M, Pan CL, Jiang GX, Zhang YM. CircRNA 010567 improves myocardial infarction rats through inhibiting TGF-β1. Eur Rev Med Pharmacol Sci. 2020;24(1):369-75.
27. Zhai C, Qian G, Wu H, Pan H, Xie S, Sun Z, et al. Knockdown of circ_0060745 alleviates acute myocardial infarction by suppressing NF-κB activation. J Cell Mol Med. 2020;24(21):12401-10.
28. Sacchetto C, Mohseni Z, Colpaert RMW, Vitiello L, De Bortoli M, Vonhögen IGC, et al. Circulating miR-185-5p as a Potential Biomarker for Arrhythmogenic Right Ventricular Cardiomyopathy. Cells. 2021;10(10).
29. Park JR, Ahn JH, Jung MH, Kim JH, Kang MG, Kim KH, et al. Serum microRNA-185 Levels and Myocardial Injury in Patients with Acute ST-segment Elevation Myocardial Infarction. Intern Med. 2022;61(2):151-8.
30. Lin R, Rahtu-Korpela L, Szabo Z, Kemppi A, Skarp S, Kiviniemi AM, et al. MiR-185-5p regulates the development of myocardial fibrosis. J Mol Cell Cardiol. 2022;165:130-40.
31. Gao F, Wang X, Fan T, Luo Z, Ma M, Hu G, et al. LncRNA LINC00461 exacerbates myocardial ischemia–reperfusion injury via microRNA-185-3p/Myd88. Molecular Medicine. 2022;28(1):33.

Figure legends:

Figure 1: CircRTN4 silencing attenuated OGD/R induced cell viability decreasing in HL-1 cells

QRT-PCR tested gene expression of circRTN4 in (A). HL-1 cells challenged by OGD/R for 1 day, (B). or with knocking down circRTN4 and challenged by OGD/R. (C). cell viability was tested in HL-1 cells knocked down with circRTN4 treated by OGD/R by CCK8. (D) cytotoxicity was tested in the same cell model by live/dead staining via flow cytometry. (E) Level of SOD and MDA in HL-1 cells from different groups were measured by commerical assays. Data presented as mean±SD. (n=3, *p<0.05, **p <0.01, ***p<0.001.)

Figure 2: CircRTN4 silencing attenuated OGD/R induced oxidative stress and inflammatory responses in HL-1 cells

(A). The protein level of cleaved Caspase-1, GSDMD-N and GAPDH were detected by western blot in HL-1 cells challenged by OGD/R with or without knocking down circRTN4. (B) The activity of caspase-1 and -4 were tested by assay kits. (C). The TNF-α, IL-1β, IL-18, and IL-10 levels from conditioned medium were tested by ELISA. Data presented as mean±SD. (n=3, *p<0.05, **p <0.01, ***p<0.001.)

Figure 3: CircRTN4 targeting miR-185 to regulate the expression level of PHLPP2

(A). Target prediction for circRTN4 to miR-185 from starBase. (B).HL-1 cells was transfected with the luciferase reporter-circRTN4 expression plasmid, and then transfected with miR-185 mimics, luciferase activity was detected by the luciferase activity kit. (C). Target prediction for miR-185 to PHLPP2, and perform the same luciferase activity assay confirmation in HL-1 cells . (D). HL-1 cells were collected, and the Ago2 and IgG were used to perform the RNA immunoprecipitation- qRT-PCR. (E). OGD/R treated HL-1 cells, and qRT-PCR was used to test the expression of miR-185. (F). Applying qRT-PCR to test the expression of miR-185 in HL-1 cells after transfecting miR-185 inhibitor. (G). HL-1 cells challenged with OGD/R with or without transfecting miR-185 inhibitor, protein was then collected and performed western blot to measure the expression level of PHLPP2. (n=3, *p<0.05, **p <0.01, ***p<0.001.)

Figure 4: Inhibition of circRTN4 attenuated cytotoxicity and inflammatory response occurred after OGD/R via miR-PHLPP2 axis

HL-1 cells transfected with circRTN4 with or without either miR-185 inhibitor or PHLPP2 ORF-clone. (A). RNA was collected from HL-1 cells after PHLPP2 ORF-clone transfection and the RNA expression level of PHLPP2 was identified by qRT-PCR. (B). Cell viability of HL-1 cells was detected by CCK8 kit from different groups, and (C). DCFH-DA assay was used to test the level of intracellular ROS. (D). The protein expression levels of cleaved caspase-1, GSDMD-N, and GAPDH were measured by western blot. (E). The activity of caspase-1 and -4 were tested by assay kits. (F). ELISA was used to measure the cytokine levels (TNF-α, IL-1β, and IL-18). Data presented as mean±SD. (n=3, *p<0.05, **p <0.01, ***p<0.001.)

Figure 5: CircRTN4 knockdown alleviated the heart tissue damage after ischemia-reperfusion injury

Mice were sacrificed after MIRI procedure, heart tissue and blood were collected. (A). Enzyme activity kits were used to measure the levels of CK-MB and LDH in serum. (B). The RNA was isolated from heart tissue, and qRT-PCR was used to detect circRTN4, miR-185, and PHLPP2 gene expression levels. (C). Heart tissue was fixed, and sections from FFPE heart tissues were used to perform the H&E staining. (D) The level of MDA from mouse serum was tested by assay kit. (E) Protein isolated from heart tissue was used to test the protein expression levels of cleaved caspase-1 and GSDMD-N, and GAPDH was used as housekeeping standard. (F). The activities of caspase-1 and caspase -4 from heart tissue were tested by assay. (G). The levels of TNF-α, IL-1β, and IL-18 from mouse serum were tested by ELISA. Data presented as mean±SD. (n=6, *p<0.05, **p <0.01, ***p<0.001.)

Figure 6. schematic drawing showing the mechanism of this study.

Fig1

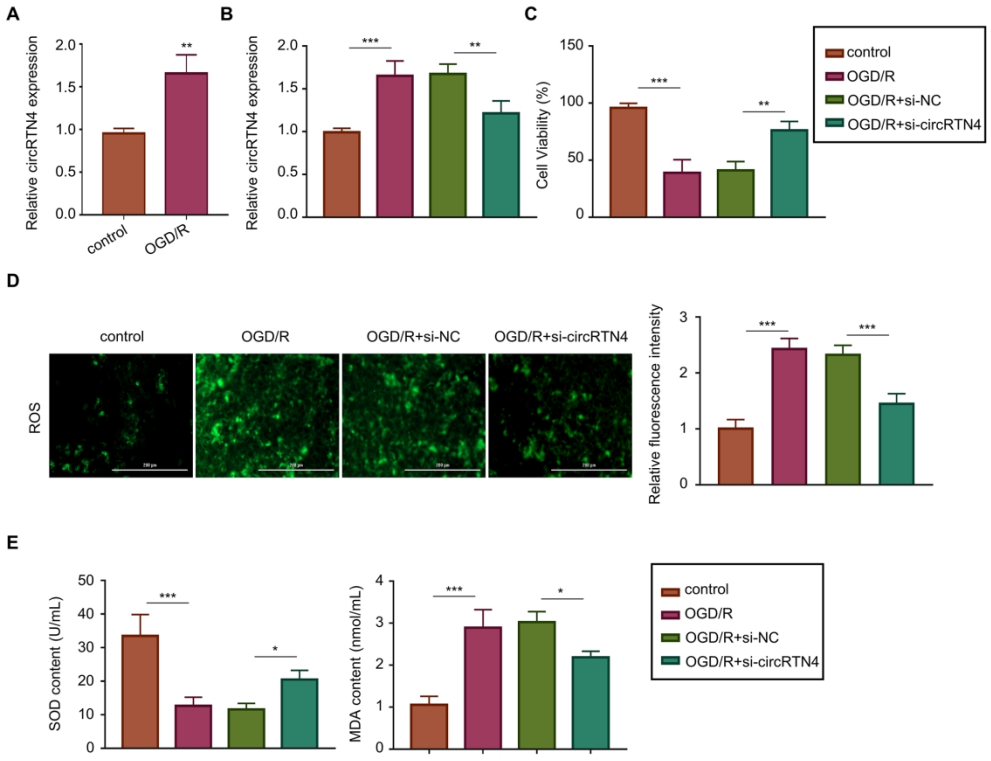

190x162mm (300 x 300 DPI)

Fig2

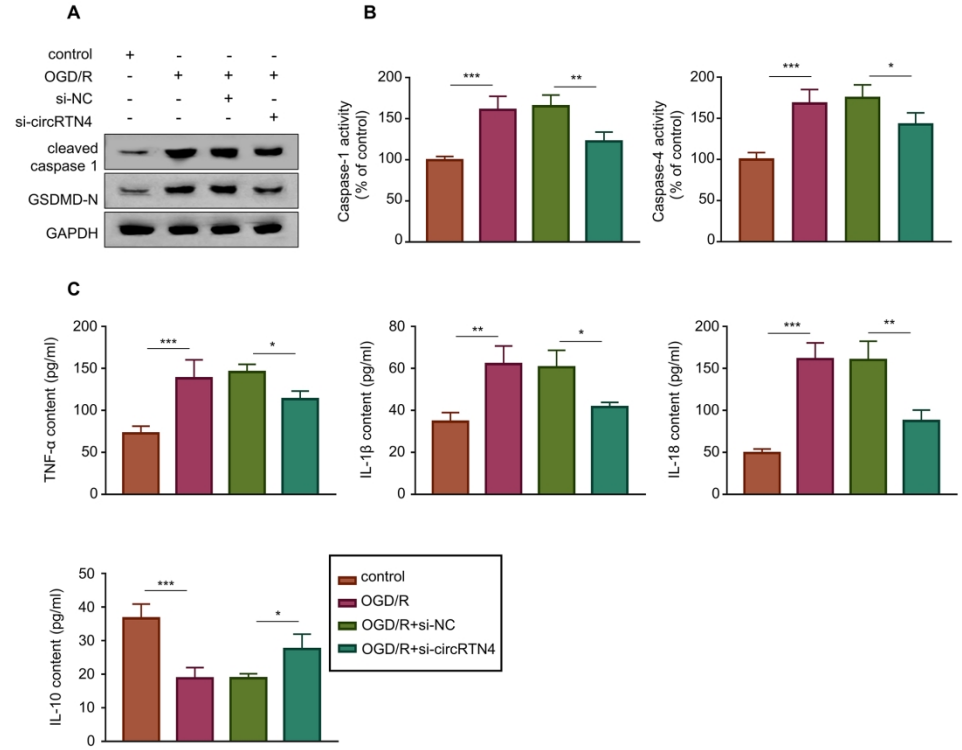

190x161mm (300 x 300 DPI)

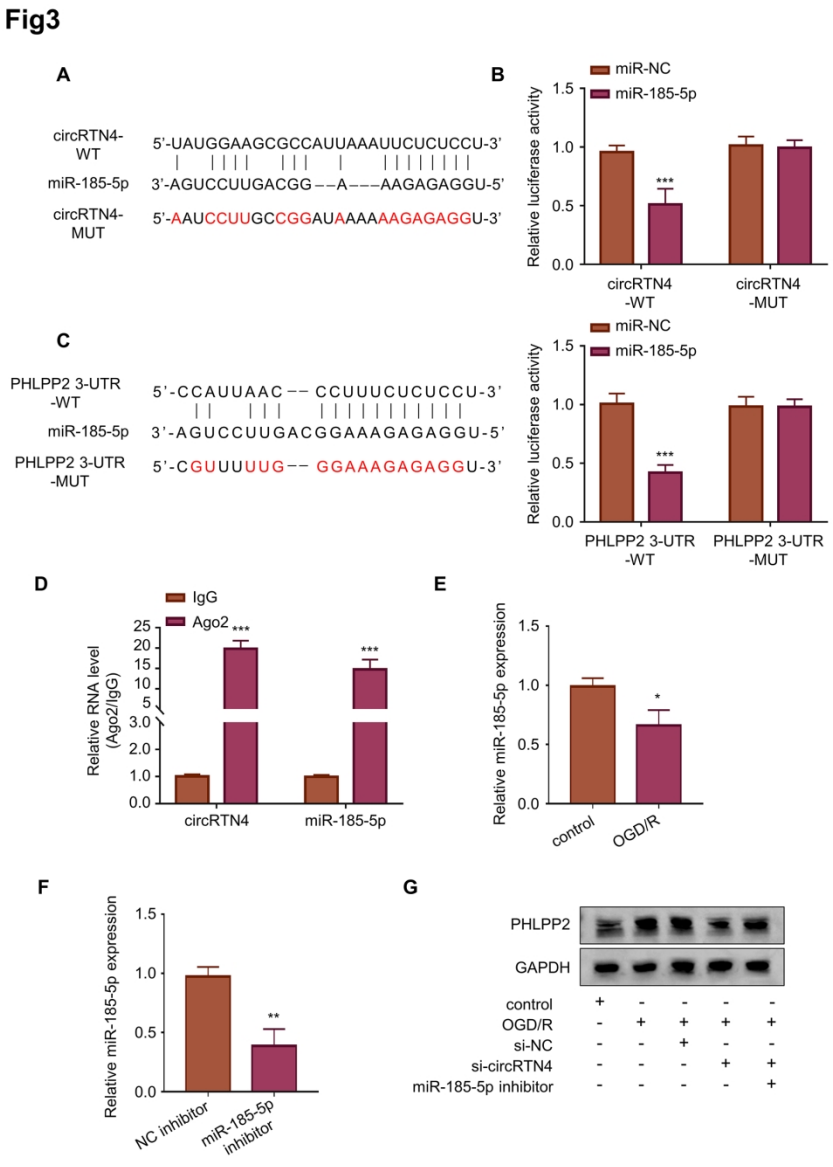

167x216mm (300 x 300 DPI)

Fig4

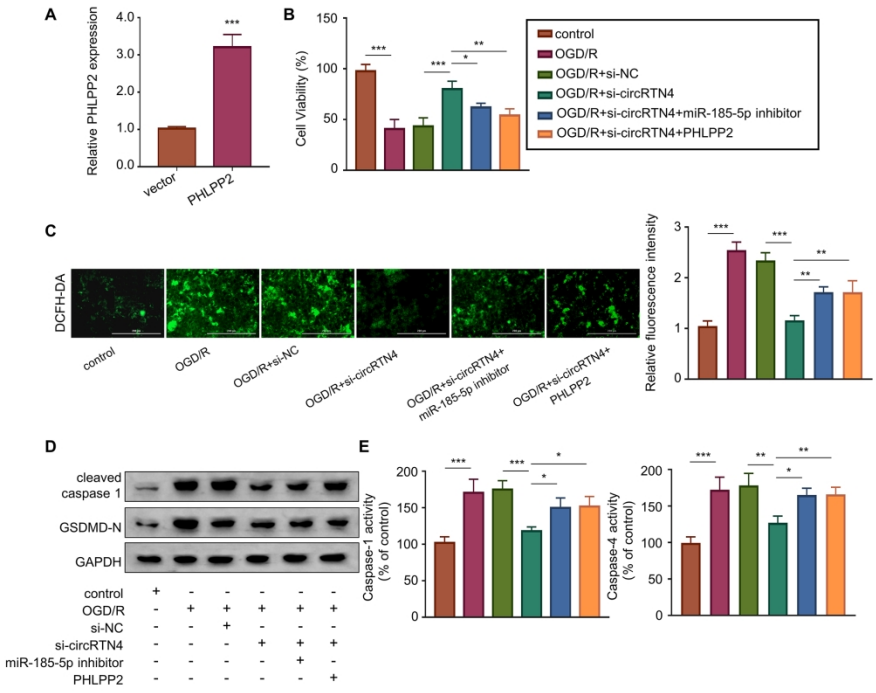

190x257mm (300 x 300 DPI)

Fig5

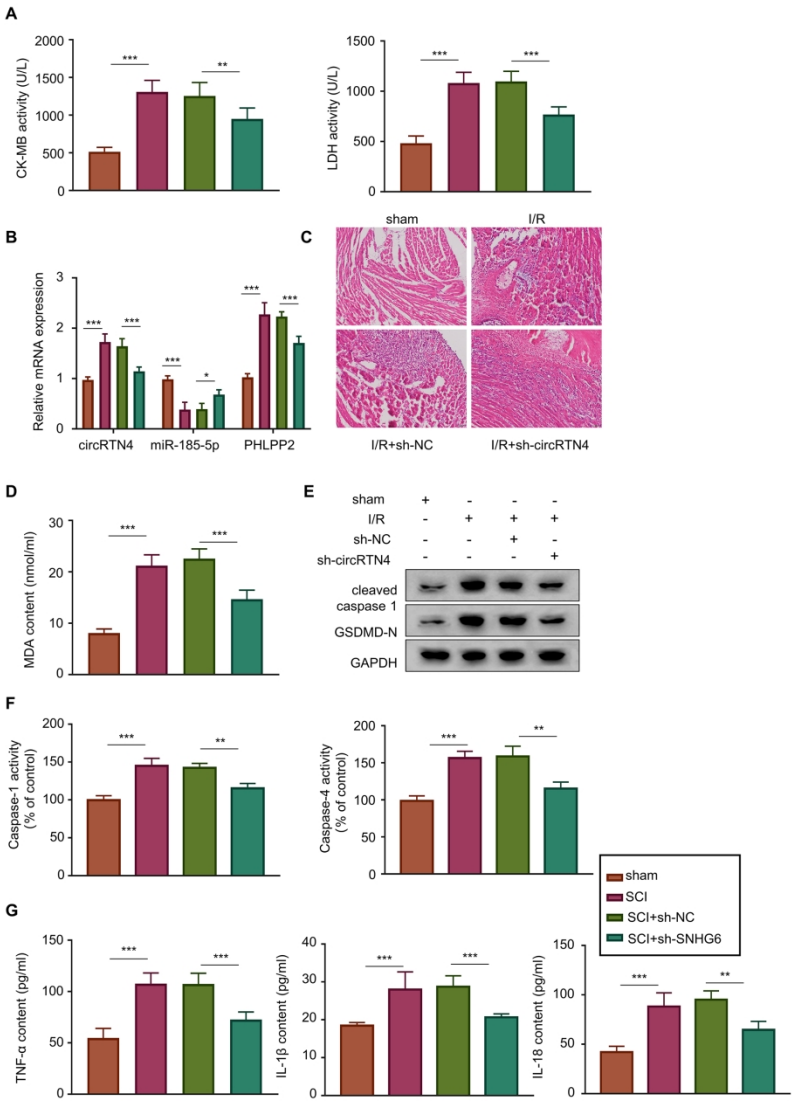

185x254mm (300 x 300 DPI)

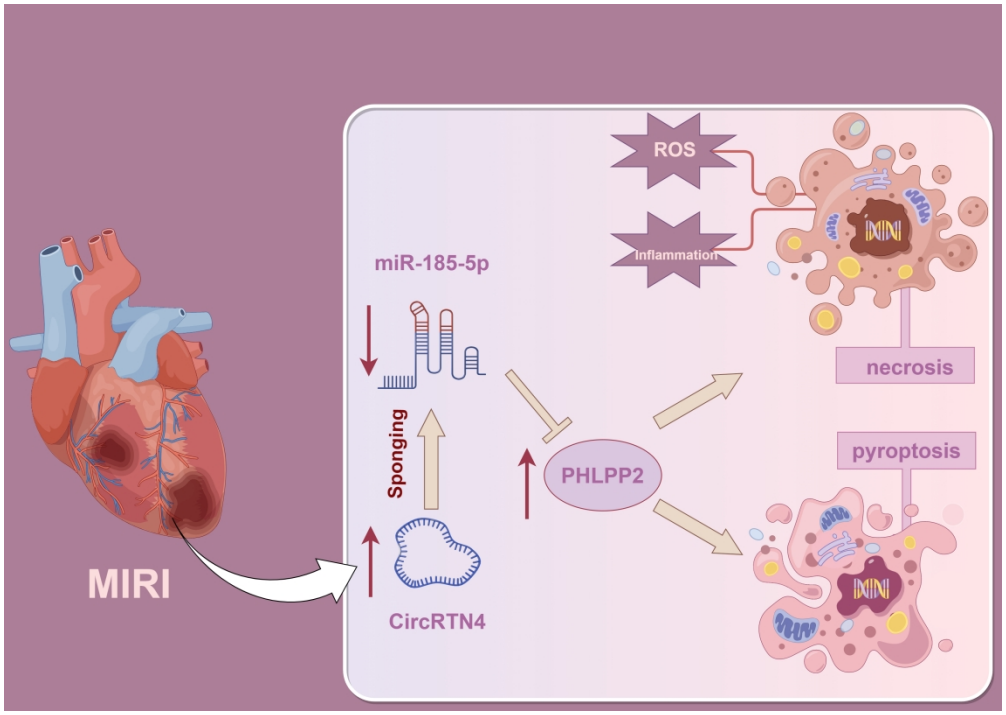

297x210mm (300 x 300 DPI)